

A Catalogue of XMM-Newton BL Lacs

Racero E.(1), de la Calle I.(2), Rouco A.(1) & Loiseau N.(2)

(1) Universidad Complutense de Madrid, Spain
(2) XMM-Newton SOC, European Space Astronomy Centre (ESAC), Spain

An XMM-Newton Catalogue of BL Lac X-ray properties is presented based on the cross-correlation with the 1374 BL Lac objects listed in the 13th edition of the Véron-Cetty & Véron Catalogue. X-ray counterparts were searched for in the field of view of around 10000 XMM-Newton pointed observations that were public before May 2013. The cross-correlation yielded a total of 330 XMM-Newton observations which correspond to 106 different potential sources. Data from the three European Photon Imaging Cameras (EPIC) and Optical Monitor (OM) were homogeneously analyzed using the latest XMM-Newton SAS software. Images, lightcurves and spectral products are produced for those sources detected in any of the three EPIC cameras. OM fluxes are computed where available. The results of the analysis are presented as a catalogue of X-ray spectral properties of the sample in the 0.2-10 keV energy band as well as in the V/UV band. Multiwavelength information at radio and high and very high gamma-ray energies complete the catalogue.

INTRODUCTION

According to the unified scheme of active galactic nuclei (AGNs), a Blazar is considered to be any radio-loud AGN that displays highly variable, beamed, non-thermal emission covering a broad range from radio to γ -ray energies. The observed rapid variability and radio properties of these objects imply that they have relativistic jets whose axes make small angles with respect to the line of sight. Low-luminosity BL Lacs (High-energy peaked BL Lacs, or HBLs) present the first peak of their SED at UV-soft/X-ray band with the second one between the GeV and the TeV band (Padovani & Giommi 1995), while their higher luminosity counterparts present the first peak around IR/Optical energies (Low-energy peaked BL Lacs, or LBLs).

In general, Blazar emission is dominated by a broad, featureless continuum, believed to originate in the relativistic jet. Observationally, the SED of Blazars, in a νF_ν representation, shows two broad distinctive peaks (Giommi & Padovani 1994). The first hump, peaking anywhere in the IR-soft X-ray range, is due to synchrotron emission, while the origin of higher energy one (usually at γ -ray frequencies) is still to be defined between processes of leptonic (Ghisellini 1999, Sikora 2001) or hadronic (Mücke 2003) nature.

The purpose of the present investigation is to contribute to the study of BL Lacs characterization by extracting the public available information on the X-ray (band pass 0.15-12 keV) and simultaneous optical/UV properties of all BL Lacs observed by XMM-Newton, whether targets or serendipitous sources in the fields.

DATA EXTRACTION AND ANALYSIS

For each source, EPIC-pn and EPIC-MOS2 source and background extraction regions are defined and optimized (Fig. 4) for spectral and lightcurve analysis.

- **EPIC:** 3CCD cameras for X-ray imaging, moderate resolution spectroscopy and X-ray photometry. The EPIC cameras have a ~ 30 arcmin field of view (FOV) with ~ 6 arcsec FWHM (Full Width Half Maximum) angular resolution and 70-80 eV energy resolution in the energy band 0.15-12keV
- Only data from EPIC and OM is considered for the catalogue

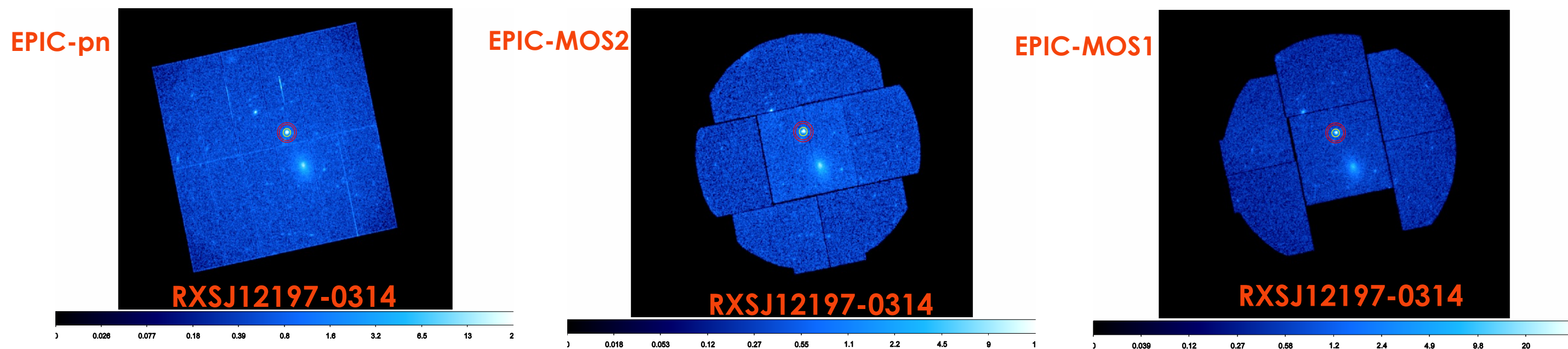


FIG. 4 Example of EPIC source and background extraction regions for product extraction

- **OM:** optical/UV imaging and spectroscopy. The OM FOV is ~ 17 arcmin FOV with ~ 1 arcsec of spatial resolution (depending on instrument configuration) and a resolving power of ~ 250 in the band pass 180-600nm. Its brightness limit is around 7.4mag.

➤ Optical Monitor (OM)

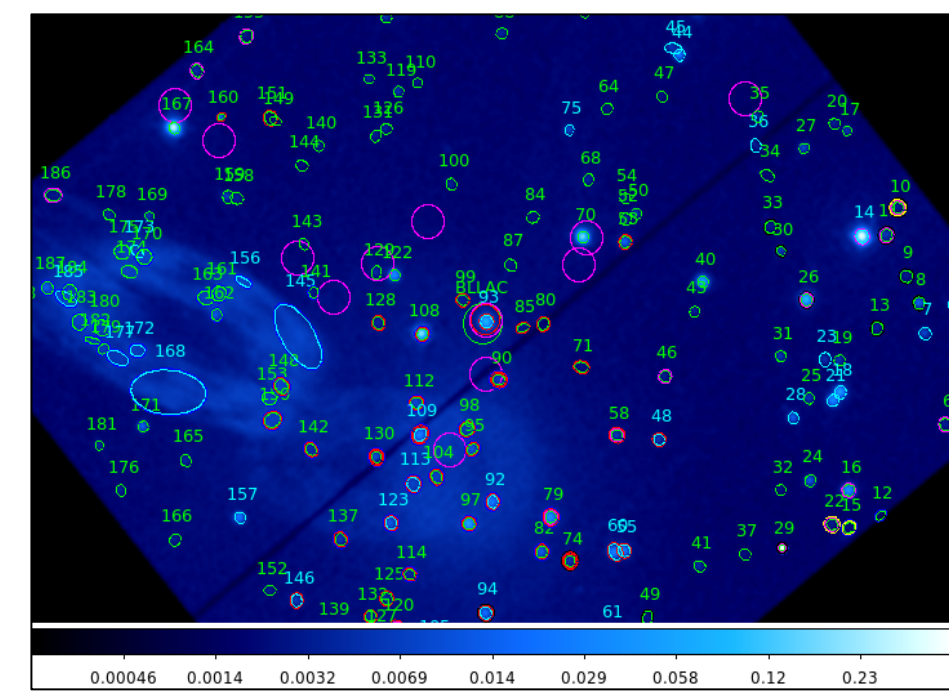


FIG. 6 OM detections

The sample has been uniformly analysed following these main steps:

1. Identification of the public XMM-Newton fields where BL Lacs from the VC&V10 Catalogue are present.
2. Reduction of these fields with the latest Science Analysis System (SAS) software (v.13.5.0) and the calibration files as to June 2014.
3. Run source detection algorithms in all selected fields, both for EPIC and OM, and cross-correlate the detected sources with the BL Lacs from the VC&V10 Catalogue.
4. For positive identifications, extract EPIC and OM images, EPIC lightcurves and spectra and OM fluxes and magnitudes.
5. With the extracted EPIC spectra, determine the best fit model and extract the best fit model parameters (Table 1). Two different models, with different variations of the column density, have been used: Log-Parabolic and Powerlaw (with fix or free column density, N_H , or both).

SUMMARY AND FUTURE WORK

- An XMM-Newton catalogue of BL Lacs X-ray properties has been produced by searching the XSA archive for X-ray counterparts of the 1374 BL Lacs listed in VC&V10 Catalogue.
- The catalogue contains around 100 sources with X-ray images, light curves and spectral information, as well as optical fluxes and magnitudes. The information will allow the classification of the BL Lacs according to their X-ray properties and to define the properties of different classes of objects.
- Variability timescales and the dependence of this variability with flux, energy or other properties could allow to disentangle the possible physical mechanisms behind.
- A statistical study is underway to try to clarify which spectral model and statistics should be used to fit spectra in an homogenous way when dealing with a sample of different statistical quality.
- The information in the catalogue, together with information at other wavelengths, will allow us to identify Blazar candidates at TeV energies.

DATA SAMPLE

The sample presented here is the result of the cross-correlation of the BL Lac sub-sample given in the Véron-Cetty & Véron Catalogue (2010, VC&C10) with all public observations available in the XMM-Newton archive up to May 2013. This BL Lac sub-sample consists of 1374 confirmed, probable or possible BL Lacs with or without a measured redshift. The initial cross-correlation is done by requesting that the VC&C10 sources fall inside any given XMM-Newton field of view. This match, yielded a total of 330 XMM-Newton observations corresponding to a potential 106 different sources (Fig. 1).

CROSS-CORRELATION XMM-NEWTON AND VC&V10 BL LAC

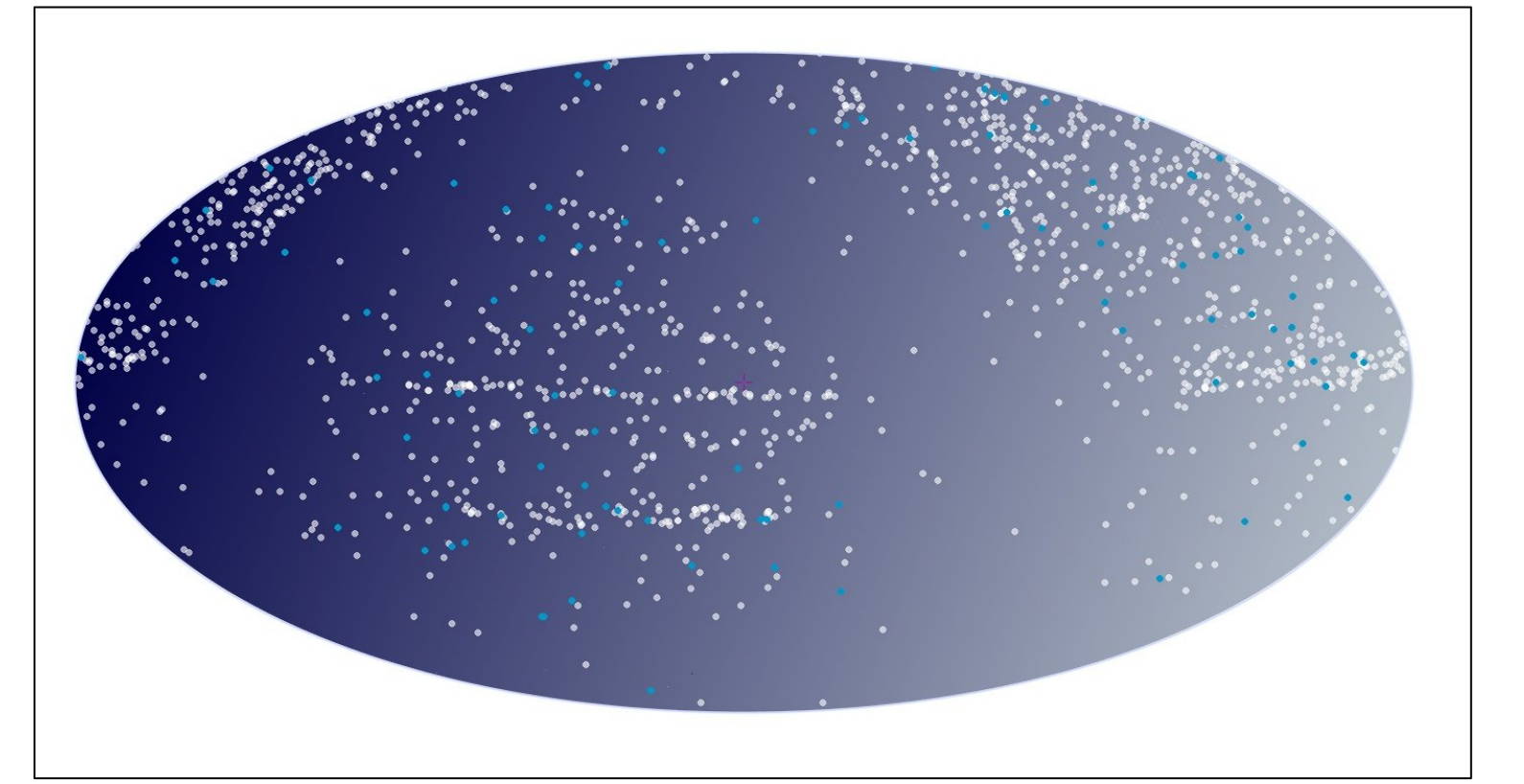


FIG. 1 In white, equatorial coordinates of VC&V10 sources. In blue, equatorial coordinates of XMM-Newton cross-correlated sources.

39/106 of the sources in our sample correspond to XMM-Newton targets while 67/106 sources are serendipitous (Fig. 2). Redshift measurements are available for 68% of the sources in the sample, with only a few percent having a redshift beyond 0.5 (Fig. 3).

Results from individual sources might have been published by individual PIs, here a uniform analysis is presented for observations focusing on the sample spectral properties.

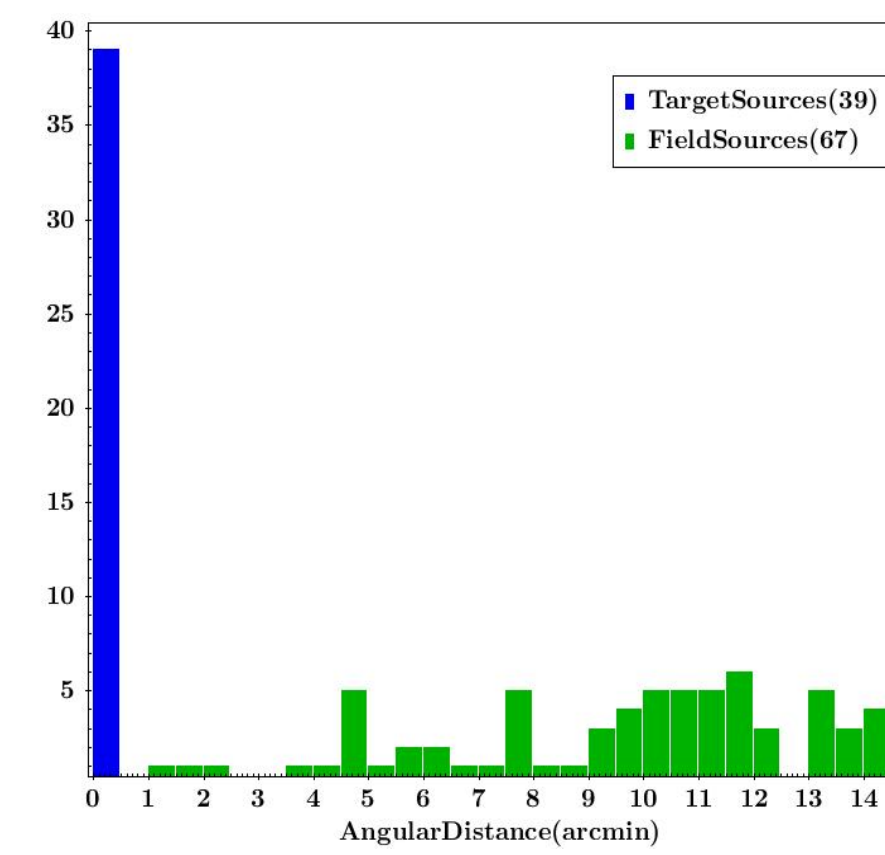
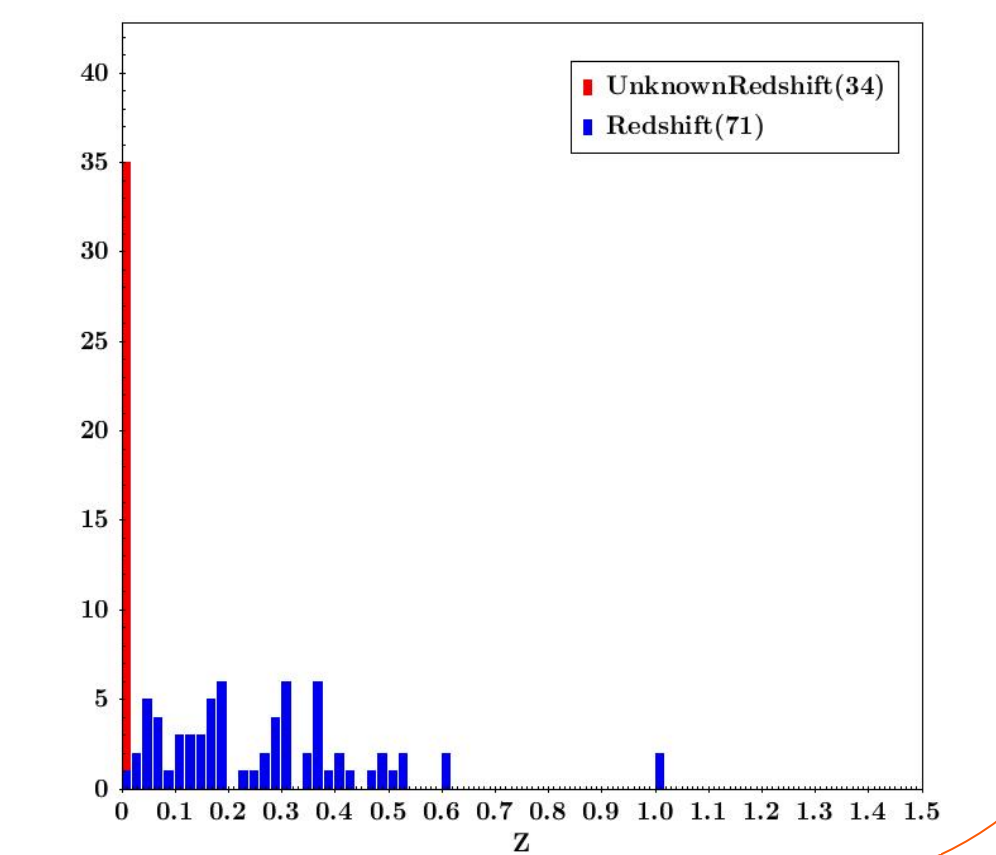


FIG. 2 Angular distance between the VC&C10 source and the target of the corresponding XMM-Newton field. (left)

FIG. 3 Redshift distribution (right)



CATALOGUE INFORMATION

Source Name	Veron Catalogue		Z	$N_{H,Gal}$	Obs ID	EPIC Source Detection					
	RA (°)	DEC (°)				Exp. (ksec)	PN (cta/sec)	MOS1 (cta/sec)	Exp. (ksec)	MOS2 (cta/sec)	
1WGAJ1108-1.7748	11h58m11.303s	-77d48m16.919s	0.351	9.05E+20	0002740501	18.3(27.86)	0.1±0	27.66(32.84)	0.04±0	27.84(32.97)	0.04±0
2QZJ113045+0035	11h30m45.288s	0d55m45.120s	0	3.08E+20	0303770601	4.368(4.368)	0.03±0	6.487(6.487)	0±0	6.492(6.492)	0.01±0
MARK180	11h36m26.495s	7d49m28.079s	0.046	1.42E+20	0094170101	6.830(11.13)	16.81±0.05	3.432(7.954)	4.07±0.04	3.266(7.771)	4.1±0.04
SDSSJ1418+0219	11h41m53.304s	2d19m23.880s	0	2.30E+20	0551750301	11.86(25.21)	0±0	24.86(30.59)	0±0	24.9(30.61)	0±0
SDSSJ12039+5819	12h3m55.296s	28d19m45.120s	0	1.45E+20	06060201	5.191(5.208)	0.05±0	7.5(7.5)	0.02±0	7.598(7.598)	0.02±0
ON231	12h21m31.704s	28d13m58.080s	0	1.88E+20	050221401	11.2(11.32)	5.73±0.03	13.51(15.83)	1.25±0.01	13.62(15.83)	1.3±0.01
3E1938+1437	19h31m29.926s	14d47m31.800s	0.760	9.51E+20	0166060201	8.548(9.277)	1.66±0.09	13.19(14.93)	0.38±0.01	13.1(14.93)	0.42±0.01
2E1228+1137	12h31m29.906s	14d21m41.890s	0.260	2.51E+20	0112550801	2.55(2.954)	2.13±0.05	13.25(13.25)	0.52±0.01	13.25(13.25)	0.46±0.01

➤ Spectra

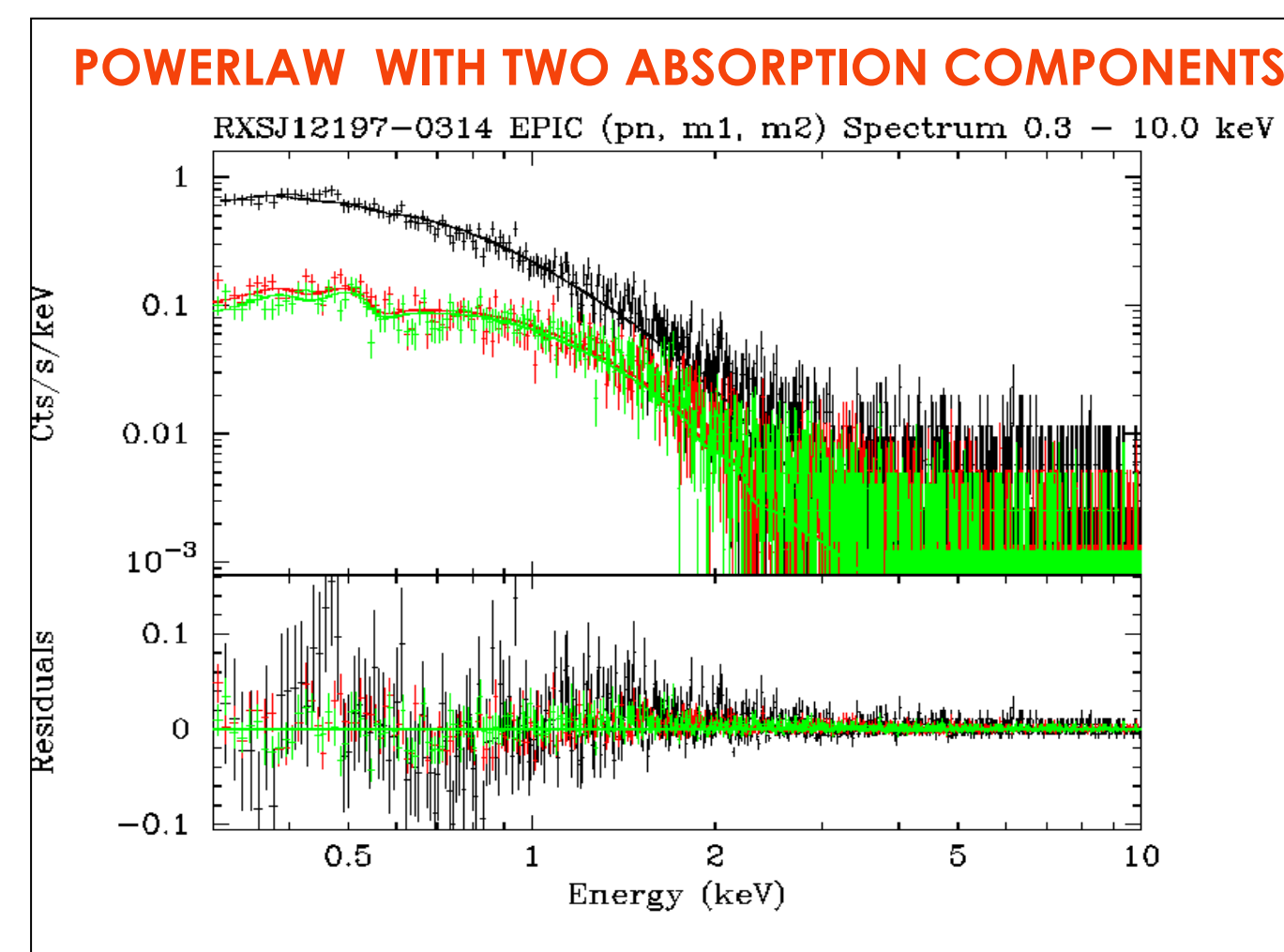


FIG. 5 Example of combined spectral fitting. EPIC-pn (black), EPIC-MOS1 (green) and EPIC-MOS2 (red) spectra. Source: RXSJ12197-0314

➤ Background Subtracted Light Curves

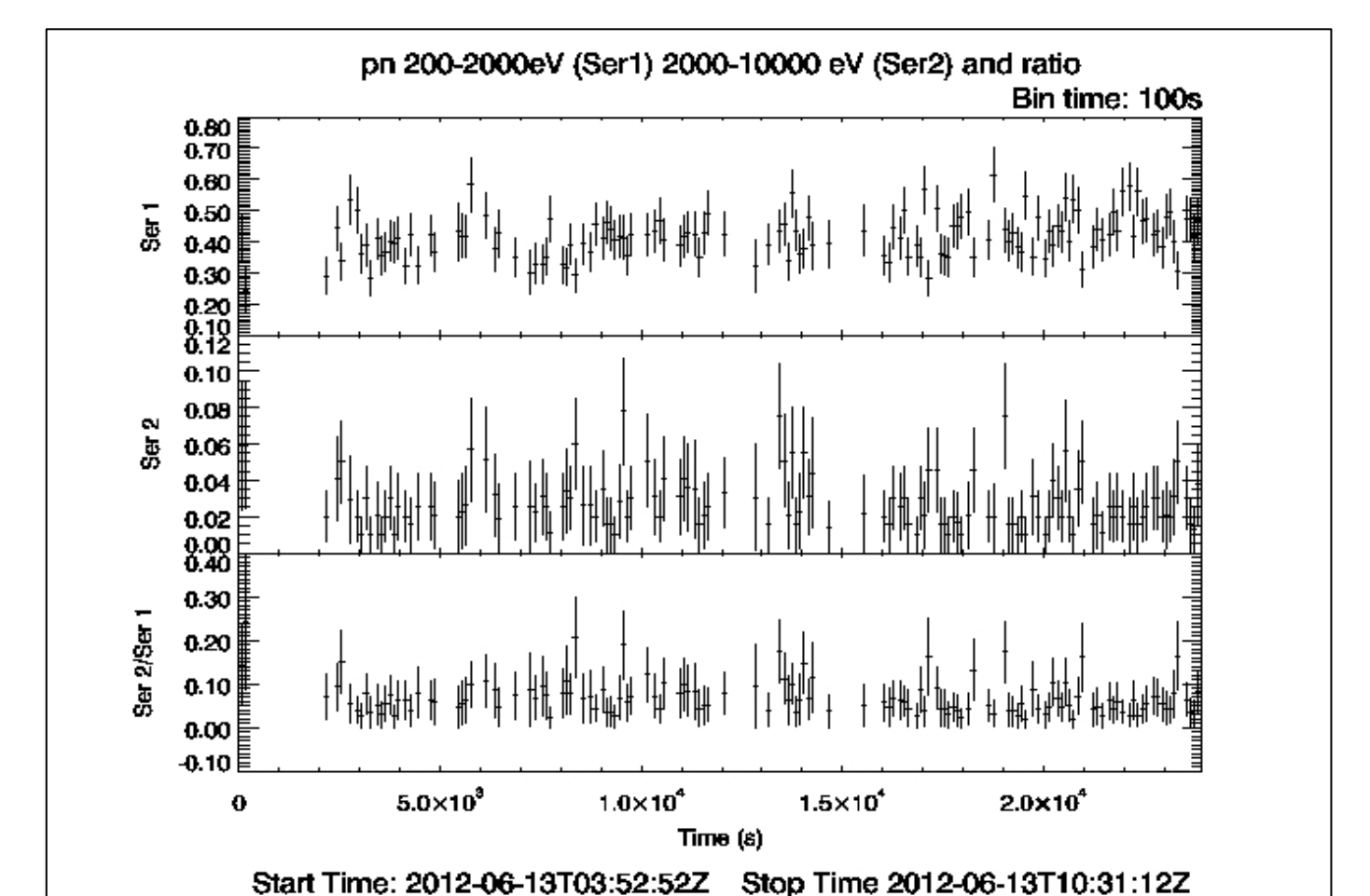


FIG. 6 Light curve in the 0.2-2 keV (top), and 2-10 keV (middle) energy ranges. Hardness ratio lightcurve (bottom). Source: RXSJ12197-0314

MODEL	N_{H}^{fix} (10^{22} g/cm 2)	N_{H}^{free} (10^{22} g/cm 2)	$N_{H}(z)$ (10^{22} g/cm 2)	α	β	$F_{0.2-10}$ (keV) (10^{-14} erg/cm 2 /s)	χ^2/DOF
PWL	N_{H}^{fix}	0.0292	-	2.7±0.01	-	0.115±0.01	1.37
	N_{H}^{free}	-	0.043±0.005	2.9±0.03	-	0.105±0.02	1.10
	$N_{H}^{fix} + N_{H}(z)$	0.0292	-	0.035±0.005	2.9±0.04	0.105±0.02	1.10
LOGPAR	N_{H}^{fix}	0.0292	-	2.40±0.04	0.34±0.05	0.105±0.002	1.13
	N_{H}^{free}	-	0.04±0.01	2.7±0.2	<0.16	0.105±0.03	1.10
	$N_{H}^{fix} + N_{H}(z)$	0.0292	-	0.03±0.01	2.7±0.2	<0.17	0.105±0.03

TABLE 1: Example best fit parameters of the combined fit to all three EPIC cameras for the different models considered.

References:

- Ghisellini, G., 1999; *Astroph. Phys.*, 11, 11
- Mücke, A., et al., 2003; *Astroph. Phys.*, 18, 593
- Padovani, P., & Giommi, P., 1995; *ApJ*, 444, 567
- Sikora, M., & Madejski, G., 2001; *AIP Conference Proc.*, 558
- Véron-Cetty, M. P., & Véron, P., 2010; *A&A*, 518, A10